Effect of the interconnected network structure on the epidemic threshold

Huijuan Wang,[1,2,*] Qian Li,[2] Gregorio D'Agostino,[3] Shlomo Havlin,[4] H. Eugene Stanley,[2] and Piet Van Mieghem[1]
[1]*Faculty of Electrical Engineering, Mathematics, and Computer Science, Delft University of Technology, Delft, The Netherlands*
[2]*Center for Polymer Studies and Department of Physics, Boston University, Boston, Massachusetts 02215, USA*
[3]*ENEA, "Casaccia" Research Center, Via Anguillarese 301, I-00123 Roma, Italy*
[4]*Department of Physics, Bar-Ilan University, 52900 Ramat-Gan, Israel*
(Received 22 March 2013; published 2 August 2013)

Most real-world networks are not isolated. In order to function fully, they are interconnected with other networks, and this interconnection influences their dynamic processes. For example, when the spread of a disease involves two species, the dynamics of the spread within each species (the contact network) differs from that of the spread between the two species (the interconnected network). We model two generic interconnected networks using two adjacency matrices, A and B, in which A is a $2N \times 2N$ matrix that depicts the connectivity within each of two networks of size N, and B a $2N \times 2N$ matrix that depicts the interconnections between the two. Using an N-intertwined mean-field approximation, we determine that a critical susceptible-infected-susceptible (SIS) epidemic threshold in two interconnected networks is $1/\lambda_1(A + \alpha B)$, where the infection rate is β within each of the two individual networks and $\alpha\beta$ in the interconnected links between the two networks and $\lambda_1(A + \alpha B)$ is the largest eigenvalue of the matrix $A + \alpha B$. In order to determine how the epidemic threshold is dependent upon the structure of interconnected networks, we analytically derive $\lambda_1(A + \alpha B)$ using a perturbation approximation for small and large α, the lower and upper bound for any α as a function of the adjacency matrix of the two individual networks, and the interconnections between the two and their largest eigenvalues and eigenvectors. We verify these approximation and boundary values for $\lambda_1(A + \alpha B)$ using numerical simulations, and determine how component network features affect $\lambda_1(A + \alpha B)$. We note that, given two isolated networks G_1 and G_2 with principal eigenvectors x and y, respectively, $\lambda_1(A + \alpha B)$ tends to be higher when nodes i and j with a higher eigenvector component product $x_i y_j$ are interconnected. This finding suggests essential insights into ways of designing interconnected networks to be robust against epidemics.

DOI: 10.1103/PhysRevE.88.022801 PACS number(s): 89.75.−k, 87.23.Ge, 89.20.−a

I. INTRODUCTION

Complex network studies have traditionally focused on single networks in which nodes represent agents and links represent the connections between agents. Recent efforts have focused on complex systems that comprise interconnected networks, a configuration that more accurately represents real-world networks [1,2]. Real-world power grids, for example, are almost always coupled with communication networks. Power stations need communication nodes for control and communication nodes need power stations for electricity. When a node at one end of an interdependent link fails, the node at the other end of the link usually fails. The influence of coupled networks on cascading failures has been widely studied [1,3–6]. A nonconsensus opinion model of two interconnected networks that allows the opinion interaction rules within each individual network to differ from those between the networks was recently studied [7]. This model shows that opinion interactions between networks can transform nonconsensus opinion behavior into consensus opinion behavior.

In this paper we investigate the susceptible-infected-susceptible (SIS) behavior of a spreading virus, a dynamic process in interconnected networks that has received significant recent attention [8–11]. An interconnected networks scenario is essential when modeling epidemics because diseases spread across multiple networks, e.g., across multiple species or communities, through both contact network links within each species or community and interconnected network links between them. Dickison *et al.* [9] study the behavior of susceptible-infected-recovered (SIR) epidemics in interconnected networks. Depending on the infection rate in weakly and strongly coupled network systems, where each individual network follows the configuration model and interconnections are randomly placed, epidemics will infect none, one, or both networks of a two-network system. Mendiola *et al.* [10] show that in SIS model an endemic state may appear in the coupled networks even when an epidemic is unable to propagate in each network separately. In this work we will explore how the structural properties of each individual network and the interconnections between them determine the epidemic threshold of two generic interconnected networks.

In order to represent two generic interconnected networks, we represent a network G with N nodes using an $N \times N$ adjacency matrix A_1 that consists of elements a_{ij}, which are either one or zero depending on whether there is a link between nodes i and j. For the interconnected networks, we consider two individual networks G_1 and G_2 of the same size N. When nodes in G_1 are labeled from 1 to N and in G_2 labeled from $N + 1$ to $2N$, the two isolated networks G_1 and G_2 can be presented by a $2N \times 2N$ matrix $A = \left[\begin{smallmatrix} A_1 & \mathbf{0} \\ \mathbf{0} & A_2 \end{smallmatrix}\right]$ composed of their corresponding adjacency matrices A_1 and A_2, respectively. Similarly, a $2N \times 2N$ matrix $B = \left[\begin{smallmatrix} \mathbf{0} & B_{12} \\ B_{12}^T & \mathbf{0} \end{smallmatrix}\right]$ represents the symmetric interconnections between G_1 and G_2. The interconnected networks are composed of three network components: network A_1, network A_2, and interconnecting network B.

In the SIS model, the state of each agent at time t is a Bernoulli random variable, where $X_i(t) = 0$ if node i is susceptible and $X_i(t) = 1$ if it is infected. The recovery

*H.Wang@tudelft.nl

(curing) process of each infected node is an independent Poisson process with a recovery rate δ. Each infected agent infects each of its susceptible neighbors with a rate β, which is also an independent Poisson process. The ratio $\tau \triangleq \beta/\delta$ is the effective infection rate. A phase transition has been observed around a critical point τ_c in a single network. When $\tau > \tau_c$, a nonzero fraction of agents will be infected in the steady state, whereas if $\tau < \tau_c$, infection rapidly disappears [12–14]. The epidemic threshold via the N-intertwined mean-field approximation (NIMFA) is $\tau_c = \frac{1}{\lambda_1(A)}$, where $\lambda_1(A)$ is the largest eigenvalue of the adjacency matrix, also called the spectral radius [15]. For interconnected networks, we assume that the curing rate δ is the same for all the nodes, that the infection rate along each link of G_1 and G_2 is β, and that the infection rate along each interconnecting link between G_1 and G_2 is $\alpha\beta$, where α is a real constant ranging within $[0,\infty)$ without losing generality.

We first show that the epidemic threshold for β/δ in interconnected networks via NIMFA is $\tau_c = \frac{1}{\lambda_1(A+\alpha B)}$, where $\lambda_1(A+\alpha B)$ is the largest eigenvalue of the matrix $A+\alpha B$. We further express $\lambda_1(A+\alpha B)$ as a function of network components A_1, A_2, and B and their eigenvalues and eigenvectors to reveal the contribution of each component network. This is a significant mathematical challenge, except for special cases, e.g., when A and B commute, i.e., $AB = BA$ (see Sec. III A). Our main contribution is that we analytically derive for the epidemic characterizer $\lambda_1(A+\alpha B)$ (a) its perturbation approximation for small α, (b) its perturbation approximation for large α, and (c) its lower and upper bound for any α as a function of component networks A_1, A_2, and B and their largest eigenvalues and eigenvectors. Numerical simulations in Sec. IV verify that these approximations and bounds well approximate $\lambda_1(A+\alpha B)$, and thus reveal the effect of component network features on the epidemic threshold of the whole system of interconnected networks, which provides essential insights into designing interconnected networks that are robust against the spread of epidemics (see Sec. V).

Sahneh *et al.* [11] recently studied SIS epidemics on generic interconnected networks in which the infection rate can differ between G_1 and G_2, and derived the epidemic threshold for the infection rate in one network while assuming that the infection does not survive in the other. Their epidemic threshold was expressed as the largest eigenvalue of a function of matrices. Our work explains how the epidemic threshold of generic interconnected networks is related to the properties (eigenvalue and eigenvector) of network components A_1, A_2, and B without any approximation on the network topology.

Graph spectra theory [16] and modern network theory, integrated with dynamic systems theory, can be used to understand how network topology can predict these dynamic processes. Youssef and Scoglio [17] have shown that an SIR epidemic threshold via NIMFA also equals $1/\lambda_1$. The Kuramoto synchronization process of coupled oscillators [18] and percolation [19] also features a phase transition that specifies the onset of a remaining fraction of locked oscillators and the appearance of a giant component, respectively. Note that a mean-field approximation predicts both phase transitions at a critical point that is proportional to $1/\lambda_1$. Thus we expect our results to apply to a wider range of dynamic processes in interconnected networks.

II. EPIDEMIC THRESHOLD OF INTERCONNECTED NETWORKS

In the SIS epidemic spreading process, the probability of infection $v_i(t) = E[X_i(t)]$ for a node i in interconnected networks G is described by

$$\frac{dv_i(t)}{dt} = \left(\beta \sum_{j=1}^{2N} a_{ij} v_j(t) + \alpha\beta \sum_{j=1}^{2N} b_{ij} v_j(t)\right) \times (1 - v_i(t)) - \delta v_i(t),$$

via NIMFA, where a_{ij} and b_{ij} is an element of matrices A and B, respectively. Its matrix form becomes

$$\frac{dV(t)}{dt} = (\beta(A+\alpha B) - \delta I)V(t) - \beta \mathrm{diag}(v_i(t))(A+\alpha B)V(t).$$

The governing equation of the SIS spreading process on a single network A_1 is

$$\frac{dV(t)}{dt} = (\beta A_1 - \delta I)V(t) - \beta \mathrm{diag}(v_i(t))A_1 V(t),$$

whose epidemic threshold has been proven [15] to be

$$\tau_c = \frac{1}{\lambda_1(A_1)},$$

which is a lower bound of the epidemic threshold [20]. Hence, the epidemic threshold of interconnected networks by NIMFA is

$$\tau_c = \frac{1}{\lambda_1(A+\alpha B)}, \tag{1}$$

which depends on the largest eigenvalue of the matrix $A+\alpha B$. The matrix $A+\alpha B$ is a weighted matrix, where $0 \leqslant \alpha < \infty$. The NIMFA is an improvement over earlier epidemic models [14] in that it takes the complete network topology into account, and thus it allows us to identify the specific role of a general network structure on the spreading process. However, NIMFA still relies on a mean-field argument and thus approximates the exact SIS epidemics [21,22].

III. ANALYTIC APPROACH: $\lambda_1(A+\alpha B)$ IN RELATION TO COMPONENT NETWORK PROPERTIES

The spectral radius $\lambda_1(A+\alpha B)$ as shown in the last section is able to characterize epidemic spreading in interconnected networks. In this section we explore how $\lambda_1(A+\alpha B)$ is influenced by the structural properties of interconnected networks and by the relative infection rate α along the interconnection links. Specifically, we express $\lambda_1(A+\alpha B)$ as a function of the component networks A_1, A_2, and B and their eigenvalues and eigenvectors. (For proofs of theorems or lemma, see the Appendix.)

A. Special cases

We start with some basic properties related to $\lambda_1(A+\alpha B)$ and examine several special cases in which the relation between $\lambda_1(A+\alpha B)$ and the structural properties of network components A_1, A_2, and B are analytically tractable.

The spectral radius of a subnetwork is always smaller or equal to that of the whole network. Hence,

Lemma 1.

$$\lambda_1(A+\alpha B) \geqslant \lambda_1(A) = \max(\lambda_1(A_1), \lambda_1(A_2)).$$

Lemma 2.

$$\lambda_1(A+\alpha B) \geqslant \alpha\lambda_1(B).$$

The interconnection network B forms a bipartite graph.

Lemma 3. The largest eigenvalue of a bipartite graph $B = \left[\begin{smallmatrix} \mathbf{0} & B_{12} \\ B_{12}^T & \mathbf{0} \end{smallmatrix}\right]$ follows $\lambda_1(B) = \sqrt{\lambda_1(B_{12}^T B_{12})}$ where B_{12} is possibly asymmetric [16].

Lemma 4. When G_1 and G_2 are both regular graphs with the same average degree $E[D]$ and when any two nodes from G_1 and G_2, respectively, are randomly interconnected with probability p_I, the average spectral radius of the interconnected networks follows:

$$E[\lambda_1(A+\alpha B)] = E[D] + \alpha N p_I,$$

if the interdependent connections are not sparse.

A dense Erdös-Rényi (ER) random network approaches a regular network when N is large. Lemma 4, thus, can be applied as well to cases where both G_1 and G_2 are dense ER random networks.

If A and B commute, thus $AB = BA$, then the eigenvectors of A and B are the same, provided that all N eigenvectors are independent [[16], p. 253]. In that case, it holds that $\lambda_1(A+B) = \lambda_1(A) + \lambda_1(B)$. This property of commuting matrices makes the following two special cases, where A and B are symmetric with orthogonal (hence, independent) eigenvectors, analytically tractable.

Lemma 5. When $A+\alpha B = \left[\begin{smallmatrix} A_1 & \mathbf{0} \\ \mathbf{0} & A_1 \end{smallmatrix}\right] + \alpha\left[\begin{smallmatrix} \mathbf{0} & I \\ I & \mathbf{0} \end{smallmatrix}\right]$, i.e., the interconnected networks are composed of two identical networks, where one network is indexed from 1 to N and the other from $N+1$ to $2N$, with an interconnecting link between each so-called image node pair $(i, N+i)$ from the two individual networks, respectively, its largest eigenvalue $\lambda_1(A+\alpha B) = \lambda_1(A) + \alpha$.

Proof. When $A+\alpha B = \left[\begin{smallmatrix} A_1 & \mathbf{0} \\ \mathbf{0} & A_1 \end{smallmatrix}\right] + \alpha\left[\begin{smallmatrix} \mathbf{0} & I \\ I & \mathbf{0} \end{smallmatrix}\right]$, matrices A and αB are commuting

$$A \cdot \alpha B = \alpha \begin{bmatrix} \mathbf{0} & A_1 \\ A_1 & \mathbf{0} \end{bmatrix} = \alpha B A.$$

Therefore, $\lambda_1(A+\alpha B) = \lambda_1(A) + \lambda_1(\alpha B) = \lambda_1(A_1) + \alpha\lambda_1(B)$. The network B is actually a set of isolated links. Hence, $\lambda_1(B) = 1$. ■

Lemma 6. When $A+\alpha B = \left[\begin{smallmatrix} A_1 & \mathbf{0} \\ \mathbf{0} & A_1 \end{smallmatrix}\right] + \alpha\left[\begin{smallmatrix} \mathbf{0} & A_1 \\ A_1 & \mathbf{0} \end{smallmatrix}\right]$, its largest eigenvalue $\lambda_1(A+\alpha B) = (1+\alpha)\lambda_1(A_1)$.

Proof. When $A+\alpha B = \left[\begin{smallmatrix} A_1 & \mathbf{0} \\ \mathbf{0} & A_1 \end{smallmatrix}\right] + \alpha\left[\begin{smallmatrix} \mathbf{0} & A_1 \\ A_1 & \mathbf{0} \end{smallmatrix}\right]$, matrices A and αB are commuting

$$A \cdot \alpha B = \alpha \begin{bmatrix} \mathbf{0} & A_1^2 \\ A_1^2 & \mathbf{0} \end{bmatrix} = \alpha B A.$$

Therefore $\lambda_1(A+\alpha B) = \lambda_1(A) + \lambda_1(\alpha B) = (1+\alpha)\lambda_1(A) = (1+\alpha)\lambda_1(A_1)$. ■

When A and B are not commuting, little can be known about the eigenvalues of $\lambda_1(A+\alpha B)$, given the spectrum of A and of B. For example, even when the eigenvalue of A and B are known and bounded, the largest eigenvalue of $\lambda_1(A+\alpha B)$ can be unbounded [16].

B. Lower bounds for $\lambda_1(A+\alpha B)$

We now denote matrix $A+\alpha B$ to be W. Applying the Rayleigh inequality [16], p. 223] to the symmetric matrix $W = A+\alpha B$ yields

$$\frac{z^T W z}{z^T z} \leqslant \lambda_1(W),$$

where equality holds only if z is the principal eigenvector of W.

Theorem 7. The best possible lower bound $\frac{z^T W z}{z^T z}$ of interdependent networks W by choosing z as the linear combination of x and y, the largest eigenvector of A_1 and A_2, respectively, is

$$\begin{aligned}\lambda_1(W) \geqslant{}& \max(\lambda_1(A_1),\lambda_1(A_2)) \\ &+ \left(\sqrt{\left(\frac{\lambda_1(A_1)-\lambda_1(A_2)}{2}\right)^2 + \xi^2}\right. \\ &\left. - \left|\frac{\lambda_1(A_1)-\lambda_1(A_2)}{2}\right|\right), \end{aligned} \tag{2}$$

where $\xi = \alpha x^T B_{12} y$.

When $\alpha = 0$, the lower bound becomes the exact solution $\lambda_1(W) = \lambda_L$. When the two individual networks have the same largest eigenvalue $\lambda_1(A_1) = \lambda_1(A_2)$, we have

$$\lambda_1(W) \geqslant \lambda_1(A_1) + \alpha x^T B_{12} y.$$

Theorem 8. The best possible lower bound $\lambda_1^2(W) \geqslant \frac{z^T W^2 z}{z^T z}$ by choosing z as the linear combination of x and y, the largest eigenvector of A_1 and A_2, respectively, is

$$\begin{aligned}&\lambda_1^2(W) \\ &\geqslant \frac{\left(\lambda_1^2(A_1) + \alpha^2\|B_{12}^T x\|_2^2 + \lambda_1^2(A_2) + \alpha^2\|B_{12} y\|_2^2\right)}{2} \\ &+ \sqrt{\left(\frac{\lambda_1^2(A_1) + \alpha^2\|B_{12}^T x\|_2^2 - \lambda_1^2(A_2) - \alpha^2\|B_{12} y\|_2^2}{2}\right)^2 + \theta^2}, \end{aligned} \tag{3}$$

where $\theta = \alpha(\lambda_1(A_1) + \lambda_1(A_2)) x^T B_{12} y$.

In general,

$$\frac{z^T W^k z}{z^T z} \leqslant \lambda_1^k(W).$$

The largest eigenvalue is lower bounded by

$$\left(\frac{z^T W^k z}{z^T z}\right)^{1/k} \leqslant \lambda_1(W).$$

Theorem 9. Given a vector z, $(\frac{z^T W^s z}{z^T z})^{1/s} \leqslant (\frac{z^T W^k z}{z^T z})^{1/k}$ when k is an even integer and $0 < s < k$. Furthermore,

$$\lim_{k\to\infty}\left(\frac{z^T W^k z}{z^T z}\right)^{1/k} = \lambda_1(W).$$

Hence, given a vector z, we could further improve the lower bound $(\frac{z^T W^k z}{z^T z})^{1/k}$ by taking a higher even power k. Note that

Theorems 7 and 8 express the lower bound as a function of component networks A_1, A_2, and B and their eigenvalues and eigenvectors, which illustrates the effect of component network features on the epidemic characterizer $\lambda_1(W)$.

C. Upper bound for $\lambda_1(A+\alpha B)$

Theorem 10. The largest eigenvalue of interdependent networks $\lambda_1(W)$ is upper bounded by

$$\lambda_1(W) \leqslant \max(\lambda_1(A_1),\lambda_1(A_2)) + \alpha\lambda_1(B) \tag{4}$$

$$= \max(\lambda_1(A_1),\lambda_1(A_2)) + \alpha\sqrt{\lambda_1\left(B_{12}B_{12}^T\right)}. \tag{5}$$

This upper bound is reached when the principal eigenvector of $B_{12}B_{12}^T$ coincides with the principal eigenvector of A_1 if $\lambda_1(A_1) \geqslant \lambda_1(A_2)$ and when the principal eigenvector of $B_{12}^T B_{12}$ coincides with the principal eigenvector of A_2 if $\lambda_1(A_1) \leqslant \lambda_1(A_2)$.

D. Perturbation analysis for small and large α

In this subsection, we derive the perturbation approximation of $\lambda_1(W)$ for small and large α, respectively, as a function of component networks and their eigenvalues and eigenvectors.

We start with small α cases. The problem is to find the largest eigenvalue $\sup_{z\neq 0}\frac{z^T W z}{z^T z}$ of W, with the condition that

$$(W-\lambda I)z = 0 \quad z^T z = 1$$

When the solution is analytical in α, we express λ and z by Taylor expansion as

$$\lambda = \sum_{k=0}^{\infty}\lambda^{(k)}\alpha^k, \quad z = \sum_{k=0}^{\infty} z^{(k)}\alpha^k.$$

Substituting the expansion in the eigenvalue equation gives

$$(A+\alpha B)\sum_{k=0}^{\infty} z^{(k)}\alpha^k = \sum_{k=0}^{\infty}\lambda^{(k)}\alpha^k \sum_{k=0}^{\infty} z^{(k)}\alpha^k,$$

where all the coefficients of α^k on the left must equal those on the right. Performing the products and reordering the series we obtain

$$\sum_{k=0}^{\infty}(Az^{(k)} + Bz^{(k-1)})\alpha^k = \sum_{k=0}^{\infty}\left(\sum_{i=0}^{k}\lambda^{(k-i)}z^{(i)}\right)\alpha^k.$$

This leads to a hierarchy of equations,

$$Az^{(k)} + Bz^{(k-1)} = \sum_{i=0}^{k}\lambda^{(k-i)}z^{(i)}.$$

The same expansion must meet the normalization condition,

$$z^T z = 1,$$

or, equivalently,

$$\left(\sum_{k=0}^{\infty} z^{(k)}\alpha^k, \sum_{j=0}^{\infty} z^{(j)}\alpha^j\right) = 1,$$

where $(u,v) = \sum_i u_i v_i$ represents the scalar product. The normalization condition leads to a set of equations,

$$\sum_{i=0}^{k}(z^{(k-i)}, z^{(i)}) = 0, \tag{6}$$

for any $k \geqslant 1$ and $(z^{(0)}, z^{(0)}) = 1$.

Let $\lambda_1(A_1)(\lambda_1(A_2))$ and $x(y)$ denote the largest eigenvalue and the corresponding eigenvector of $A_1(A_2)$, respectively. We examine two possible cases: (a) the nondegenerate case when $\lambda_1(A_1) > \lambda_1(A_2)$ and (b) the degenerate case when $\lambda_1(A_1) = \lambda_1(A_2)$ and the case $\lambda_1(A_1) < \lambda_1(A_2)$ is equivalent to the first.

Theorem 11. For small α, in the nondegenerate case, thus when $\lambda_1(A_1) > \lambda_1(A_2)$,

$$\lambda_1(W) = \lambda_1(A_1) + \alpha^2 x^T B_{12}(\lambda_1(A_1)I - A_2)^{-1}B_{12}^T x + O(\alpha^3). \tag{7}$$

Note that in (A6) B is symmetric and $(\lambda^{(0)}I - A)$ is positive definite and so is $B(\lambda^{(0)}I - A)^{-1}B$. Hence, this second-order correction $\lambda^{(2)}$ is always positive.

Theorem 12. For small α, when the two component networks have the same largest eigenvalue $\lambda_1(A_1) = \lambda_1(A_2)$,

$$\begin{aligned}\lambda_1(W) = {} & \lambda^{(0)} + \alpha\lambda^{(1)} + \frac{1}{2}\alpha^2 y^T B_{12}^T\left(\lambda^{(0)}I - A_1 + \frac{1}{2}xx^T\right)^{-1} \\ & \times (B_{12}y - \lambda^{(1)}x) + \frac{1}{2}\alpha^2 x^T B_{12} \\ & \times \left(\lambda^{(0)}I - A_2 + \frac{1}{2}yy^T\right)^{-1}\left(B_{12}^T x - \lambda^{(1)}y\right) + O(\alpha^3),\end{aligned} \tag{8}$$

where $\lambda^{(0)} = \lambda_1(A_1)$ and $\lambda^{(1)} = x^T B_{12} y$.

In the degenerate case, the first-order correction is positive and the slope depends on B_{12}, y, and x. When A_1 and A_2 are identical, the largest eigenvalue of the interdependent networks becomes

$$\lambda = \lambda_1(A_1) + \alpha(B_{12}x, x) + O(\alpha^2).$$

When $A = \left[\begin{smallmatrix} A_1 & \mathbf{0} \\ \mathbf{0} & A_1 \end{smallmatrix}\right]$ and $B = \left[\begin{smallmatrix} \mathbf{0} & I \\ I & \mathbf{0} \end{smallmatrix}\right]$, our result (8) in the degenerate case up to the first order leads to $\lambda_1(A+\alpha B) = \lambda_1(A) + \alpha$, which is an alternate proof of Lemma 5. When $A = \left[\begin{smallmatrix} A_1 & \mathbf{0} \\ \mathbf{0} & A_1 \end{smallmatrix}\right]$ and $B = \left[\begin{smallmatrix} \mathbf{0} & A_1 \\ A_1 & \mathbf{0} \end{smallmatrix}\right]$, (8) again explains Lemma 6 that $\lambda_1(A+\alpha B) = (1+\alpha)\lambda_1(A_1)$.

Lemma 13. For large α, the spectral radius of interconnected networks is

$$\lambda_1(A+\alpha B) = \alpha\lambda_1(B) + v^T A v + O(\alpha^{-1}), \tag{9}$$

where v is the eigenvector belonging to $\lambda_1(B)$ and

$$\lambda_1(A+\alpha B) \leqslant \lambda_1(A) + \alpha\lambda_1(B) + O(\alpha^{-1}).$$

Proof. Lemma 13 follows by applying perturbation theory [23] to the matrix $\alpha(B + \frac{1}{\alpha}A)$ and the Rayleigh principle [16], which states that $v^T A v \leqslant \lambda_1(A)$, for any normalized vector v such that $v^T v = 1$, with equality only if v is the eigenvector belonging to the eigenvalue $\lambda_1(A)$. ■

IV. NUMERICAL SIMULATIONS

In this section, we employ numerical calculations to quantify to what extent the perturbation approximation (7) and (8) for small α, the perturbation approximation (9) for large α, and the upper (4) and lower bound (3) are close to the exact value $\lambda_1(W) = \lambda_1(A + \alpha B)$. We investigate the condition under which the approximations provide better estimates. The analytical results derived earlier are valid for arbitrary interconnected network structures. For simulations, we consider two classic network models as possible topologies of G_1 and G_2: (i) the Erdös-Rényi (ER) random network [24–26] and (ii) the Barabási-Albert (BA) scale-free network [27]. ER networks are characterized by a binomial degree distribution $\Pr[D = k] = \binom{N-1}{k} p^k (1-p)^{N-1-k}$, where N is the size of the network and p is the probability that each node pair is randomly connected. In scale-free networks, the degree distribution is given by a power law $\Pr[D = k] = ck^{-\lambda}$ such that $\sum_{k=1}^{N-1} ck^{-\lambda} = 1$ and $\lambda = 3$ in BA scale-free networks.

In numerical simulations, we consider $N_1 = N_2 = 1000$. Specifically, in the BA scale-free networks $m = 3$ and the corresponding link density is $p_{\mathrm{BA}} \simeq 0.006$. We consider ER networks with the same link density $p_{\mathrm{ER}} = p_{\mathrm{BA}} = 0.006$. A coupled network G is the union of G_1 and G_2, which are chosen from the above-mentioned models, together with random interconnection links with density p_I, the probability that any two nodes from G_1 and G_2, respectively, are interconnected. Given the network models of G_1 and G_2 and the interacting link density p_I, we generate 100 interconnected network realizations. For each realization, we compute the spectral radius $\lambda_1(W)$, its perturbation approximation (7) and (8) for small α, the perturbation approximation (9) for large α, and the upper bound (4) and lower bound (3) for any α. We compare their averages over the 100 coupled network realizations. We investigate the degenerate case $\lambda_1(G_1) = \lambda_1(G_2)$ where the largest eigenvalues of G_1 and G_2 are the same and the nondegenerate case where $\lambda_1(G_1) \neq \lambda_1(G_2)$, respectively.

A. Nondegenerate case

We consider the nondegenerate case in which G_1 is a BA scale-free network with $N = 1000, m = 3$, G_2 is an ER random network with the same size and link density $p_{\mathrm{ER}} = p_{\mathrm{BA}} \simeq 0.006$, and the two networks are randomly interconnected with link density p_I. We compute the largest average eigenvalue $E[\lambda_1(W)]$ and the average of the perturbation approximations and bounds mentioned above over 100 interconnected network realizations for each interconnection link density $p_I \in [0.00025, 0.004]$ such that the average number of interdependent links ranges from $\frac{N}{4}, \frac{N}{2}, N, 2N$ to $4N$ and for each value α that ranges from 0 to 10 with step size 0.05.

For a single BA scale-free network, where the power exponent $\beta = 3 > 2.5$, the largest eigenvalue is $(1 + o(1))\sqrt{d_{\max}}$ where $d_{\max}$ is the maximum degree in the network [28]. The spectral radius of a single ER random graph is close to the average degree $(N-1)p_{\mathrm{ER}}$ when the network is not sparse. When $p_I = 0$, $\lambda_1(G) = \max(\lambda_1(G_{\mathrm{ER}}), \lambda_1(G_{\mathrm{BA}})) = \lambda_1(G_{\mathrm{BA}}) > \lambda_1(G_{ER})$. The perturbation approximation is expected to be close to the exact $\lambda_1(W)$ only for $\alpha \to 0$ and $\alpha \to \infty$. However, as shown in Fig. 1(a), the perturbation approximation for small α approximates $\lambda_1(W)$ well for a relative large range of α, especially for sparser interconnections, i.e., for a smaller interconnection density p_I. Figure 1(b) shows that the exact spectral radius $\lambda_1(W)$ is already close to the large α perturbation approximation, at least for $\alpha > 8$.

As depicted in Fig. 2, the lower bound (3) and upper bound (4) are sharp, i.e., close to $\lambda_1(W)$ for small α. The lower and upper bounds are the same as $\lambda_1(W)$ when $\alpha \to 0$. For large α, the lower bound better approximates $\lambda_1(W)$ when the interconnections are sparser. Another lower bound $\alpha\lambda_1(B) \leqslant \lambda_1(W)$, i.e., Lemma 2, is sharp for large α, as shown in Fig. 3, especially for sparse interconnections. We do not illustrate the lower bound (2) because the lower bound (3) is always sharper or equally good. The lower bound $\alpha\lambda_1(B)$ considers only the largest eigenvalue of the interconnection network B and ignores the two individual networks G_1 and G_2. The difference

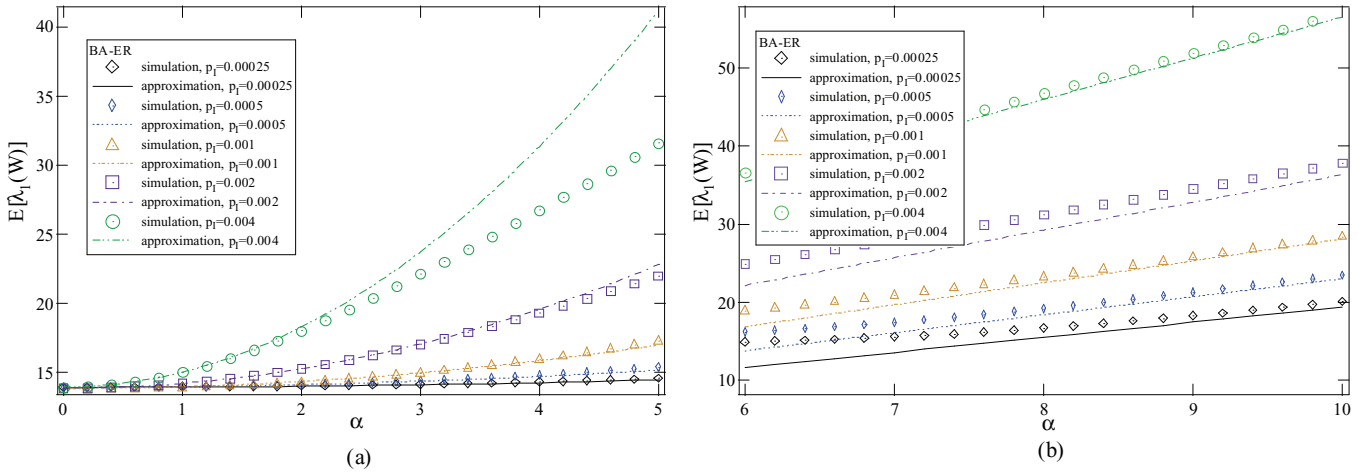

FIG. 1. (Color online) A plot of $\lambda_1(W)$ as a function of α for both simulation results (symbol) and its (a) perturbation approximation (7) for small α (dashed line) and (b) perturbation approximation (9) for large α (dashed line). The interconnected network is composed of an ER random network and a BA scale-free network both with $N = 1000$ and link density $p = 0.006$, randomly interconnected with density p_I. All the results are averages of 100 realizations.

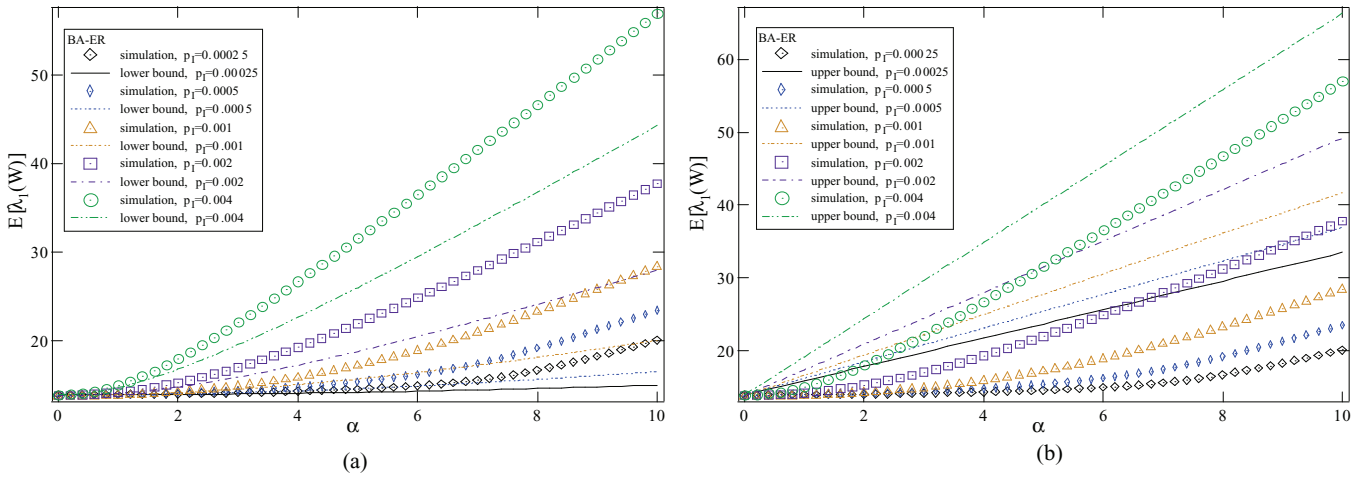

FIG. 2. (Color online) Plot $\lambda_1(W)$ as a function of α for both simulation results (symbol) and its (a) lower bound (3) (dashed line) and (b) upper bound (4) (dashed line). The interconnected network is composed of an ER random network and a BA scale-free network both with $N = 1000$ and link density $p = 0.006$, randomly interconnected with density p_I. All the results are averages of 100 realizations.

$\lambda_1(W) - \alpha\lambda_1(B) = v^T A v + O(\alpha^{-1})$ according to the large α perturbation approximation, is shown in Fig. 3 to be larger for denser interconnections. It suggests that G_1 and G_2 contribute more to the spectral radius of the interconnected networks when the interconnections are denser in this nondegenerate case. For large α, the upper bound is sharper when the interconnections are denser or when p_I is larger, as depicted in Fig. 2(b). This is because $\alpha\lambda_1(B) \leqslant \lambda_1(W) \leqslant \alpha\lambda_1(B) + \max(\lambda_1(A_1), \lambda_1(A_2))$. When the interconnections are sparse, $\lambda_1(W)$ is close to the lower bound $\alpha\lambda_1(B)$ and hence far from the upper bound.

Most interdependent or coupled networks studied so far assume that both individual networks have the same number of nodes N and that the two networks are interconnected randomly by N one-to-one interconnections, or by a fraction q of the N one-to-one interconnections where $0 < q \leqslant 1$ [1,6,7]. These coupled networks correspond to our sparse interconnection cases where $p_I \leqslant 1$, when $\lambda_1(B)$ is well approximated by the perturbation approximation for both small and large α. The spectral radius $\lambda_1(W)$ increases quadratically with α for small α, as described by the small α perturbation approximation. The increase accelerates as α increases and converges to a linear increase with α, with slope $\lambda_1(B)$. Here we show the cases in which G_1, G_2, and the interconnections are sparse, as in most real-world networks. However, all the analytical results can be applied to arbitrary interconnected network structures.

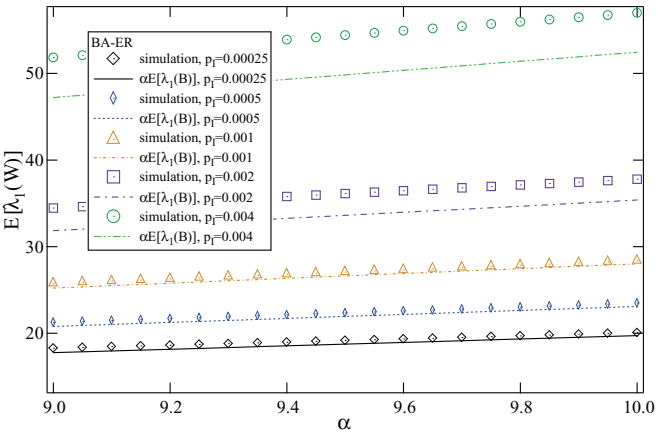

FIG. 3. (Color online) Plot $\lambda_1(W)$ as a function of α for both simulation results (symbol) and its lower bound $\alpha\lambda_1(B)$ (dashed line). The interconnected network is composed of an ER random network and a BA scale-free network both with $N = 1000$ and link density $p = 0.006$, randomly interconnected with density p_I. All the results are averages of 100 realizations.

B. Degenerate case

We assume the spectrum [29] to be a unique fingerprint of a large network. Two large networks of the same size seldom have the same largest eigenvalue. Hence, most interconnected networks belong to the nondegenerate case. Degenerate cases mostly occur when G_1 and G_2 are identical, or when they are both regular networks with the same degree. We consider two degenerate cases where both network G_1 and G_2 are ER random networks or BA scale-free networks. Both ER and BA networks lead to the same observations. Hence as an example we show the case in which both G_1 and G_2 are BA scale-free networks of size $N = 1000$ and both are randomly interconnected with density $p_I \in [0.00025, 0.004]$, as in the nondegenerate case. Figure 4(a) shows that the perturbation analysis well approximates $\lambda_1(W)$ for small α, especially when the interconnection density is small. When the interconnections are dense, the small α perturbation approximation performs better in the degenerate case, i.e., is closer to $\lambda_1(W)$ than in nondegenerate cases [see Fig. 1(a)]. Similar to the nondegenerate case, Fig. 4(b) illustrates that the exact spectral radius $\lambda_1(W)$ is close to the large α perturbation approximation even since $\alpha = 8$.

Similarly, Fig. 5 shows that both the lower and upper bound are sharper for small α. The lower bound better approximates $\lambda_1(W)$ for sparser interconnections whereas the upper bound better approximates $\lambda_1(W)$ for denser interconnections.

Thus far we have examined the cases where G_1, G_2, and the interconnections are sparse, as is the case in most real-world networks. However, if both G_1 and G_2 are dense

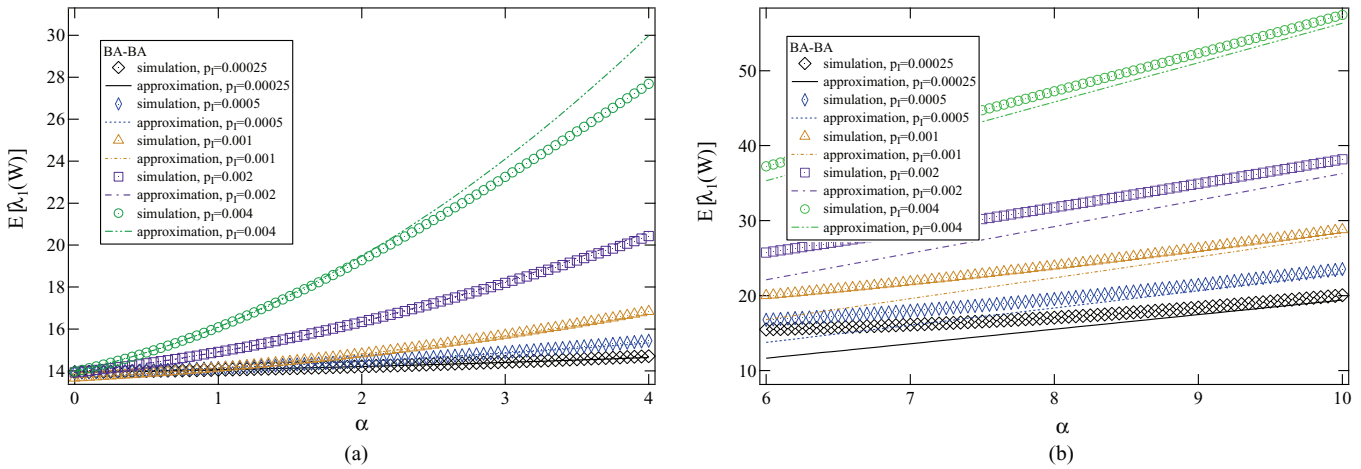

FIG. 4. (Color online) A plot of $\lambda_1(W)$ as a function of α for both simulation results (symbol) and its (a) perturbation approximation (8) for small α (dashed line) and (b) perturbation approximation (9) for large α (dashed line). The interconnected network is composed of two identical BA scale-free networks with $N = 1000$ and link density $p = 0.006$, randomly interconnected with density p_I. All the results are averages of 100 realizations.

ER random networks and if the random interconnections are also dense, the upper bound is equal to $\lambda_1(W)$, i.e., $\lambda_1(W) = \lambda_1(G_1) + \alpha\lambda_1(B)$ (see Lemma 4). Equivalently, the difference $\lambda_1(W) - \alpha\lambda_1(B)$ is a constant $\lambda_1(G_1) = \lambda_1(G_2)$ independent of the interconnection density p_I.

In both the nondegenerate and degenerate case, $\lambda_1(W)$ is well approximated by a perturbation analysis for a large range of α, especially when the interconnections are sparse. The lower bound (3) and upper bound (4) are sharper for small α. Most real-world networks are sparsely interconnected, where our perturbation analysis better approximates $\lambda_1(W)$ for a large range of α, and thus well reveals the effect of component network structures on the epidemic characterizer $\lambda_1(W)$.

V. CONCLUSION

We study interconnected networks that are composed of two individual networks G_1 and G_2, and interconnecting links represented by adjacency matrices A_1, A_2, and B, respectively. We consider SIS epidemic spreading in these generic coupled networks, where the infection rate within G_1 and G_2 is β, the infection rate between the two networks is $\alpha\beta$, and the recovery rate is δ for all agents. Using a NIMFA we show that the epidemic threshold with respect to β/δ is $\tau_c = \frac{1}{\lambda_1(A+\alpha B)}$, where $A = \left[\begin{smallmatrix} A_1 & \mathbf{0} \\ \mathbf{0} & A_2 \end{smallmatrix}\right]$ is the adjacency matrix of the two isolated networks G_1 and G_2. The largest eigenvalue $\lambda_1(A + \alpha B)$ can thus be used to characterize epidemic spreading. This eigenvalue $\lambda_1(A + \alpha B)$ of a function of matrices seldom gives the contribution of each component network. We analytically express the perturbation approximation for small and large α, lower and upper bounds for any α, of $\lambda_1(A + \alpha B)$ as a function of component networks A_1, A_2, and B and their largest eigenvalues and eigenvectors. Using numerical simulations, we verify that these approximations or bounds approximate well the exact $\lambda_1(A + \alpha B)$, especially when the interconnections are sparse, as is the case in most real-world interconnected

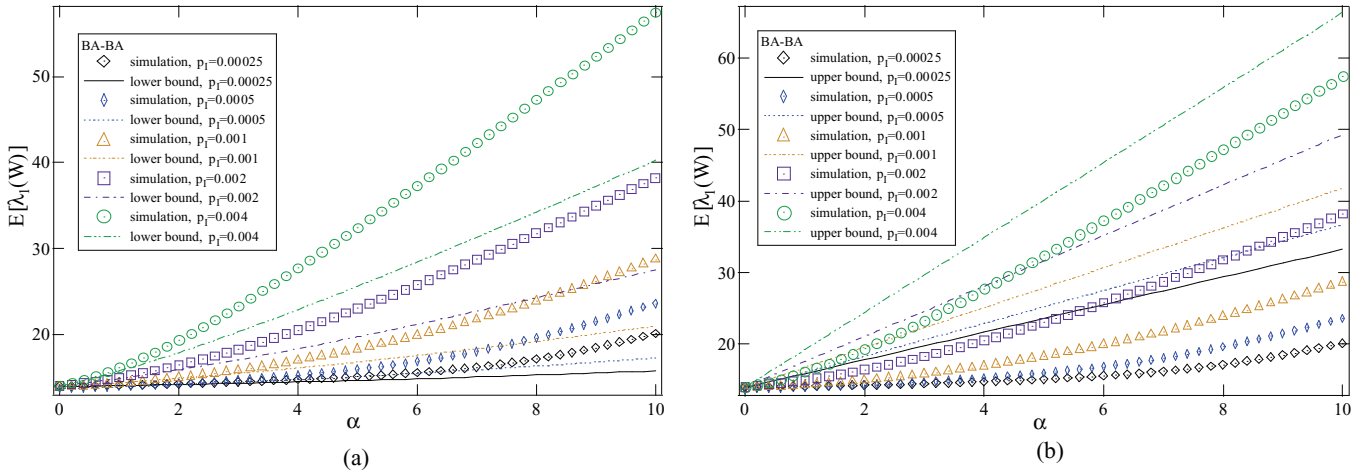

FIG. 5. (Color online) Plot $\lambda_1(W)$ as a function of α for both simulation results (symbol) and (a) its lower bound (3) (dashed line) and (b) upper bound (4) (dashed line). The interconnected network is composed of two identical BA scale-free networks $N = 1000$ and link density $p = 0.006$, randomly interconnected with density p_I. All the results are averages of 100 realizations.

networks. Hence, these approximations and bounds reveal how component network properties affect the epidemic characterizer $\lambda_1(A+\alpha B)$. Note that the term $x^T B_{12} y$ contributes positively to the perturbation approximation (8) and the lower bound (3) of $\lambda_1(A+\alpha B)$ where x and y are the principal eigenvector of network G_1 and G_2. This suggests that, given two isolated networks G_1 and G_2, the interconnected networks have a larger $\lambda_1(A+\alpha B)$ or a smaller epidemic threshold if the two nodes i and j with a larger eigenvector component product $x_i y_j$ from the two networks, respectively, are interconnected. This observation provides essential insights useful when designing interconnected networks to be robust against epidemics. The largest eigenvalue also characterizes the phase transition of coupled oscillators and percolation. Our results apply to arbitrary interconnected network structures and are expected to apply to a wider range of dynamic processes.

ACKNOWLEDGMENTS

We wish to thank ONR (Grants No. N00014-09-1-0380 and No. N00014-12-1-0548), DTRA (Grants No. HDTRA-1-10-1-0014 and No. HDTRA-1-09-1-0035), NSF (Grant No. CMMI 1125290), the European EPIWORK, MULTIPLEX, CONGAS (Grant No. FP7-ICT-2011-8-317672), MOTIA (Grant No. JLS-2009-CIPS-AG-C1-016), and LINC projects, the Deutsche Forschungsgemeinschaft (DFG), the Next Generation Infrastructure (Bsik), and the Israel Science Foundation for financial support.

APPENDIX: PROOFS

1. Proof of Lemma 4

In any regular graph, the minimal and maximal node strength are both equal to the average node strength. Since the largest eigenvalue is lower bounded by the average node strength and upper bounded by the maximal node strength as proved below in Lemma 14, a regular graph has the minimal possible spectral radius, which equals the average node strength. When the interdependent links are randomly connected with link density p_I, the coupled network is asymptotically a regular graph with average node strength $E[D]+\alpha N p_I$, if p_I is a constant.

Lemma 14. For any $N \times N$ weighted symmetric matrix W,

$$E[S] \leqslant \lambda_1(W) \leqslant \max s_r,$$

where $s_r = \sum_{j=1}^{N} w_{rj}$ is defined as the node strength of node r and $E[S]$ is the average node strength over all the nodes in graph G.

Proof. The largest eigenvalue λ_1 follows:

$$\lambda_1 = \sup_{x \neq 0} \frac{x^T W x}{x^T x},$$

when matrix W is symmetric and the maximum is attained if and only if x is the eigenvector of W belonging to $\lambda_1(W)$. For any other vector $y \neq x$, it holds that $\lambda_1 \geqslant \frac{y^T W y}{y^T y}$. By choosing the vector $y = u = (1,1,\ldots,1)$, we have

$$\lambda_1 \geqslant \frac{1}{N}\sum_{i=1}^{N}\sum_{j=1}^{N} w_{ij} = \frac{1}{N}\sum_{i=1}^{N} s_i = E[S],$$

where w_{ij} is the element in matrix W and $E[S]$ is the average node strength of the graph G. The upper bound is proved by the Gerschgorin circle theorem. Suppose component r of eigenvector x has the largest modulus. The eigenvector can be always normalized such that

$$x' = \left(\frac{x_1}{x_r}, \frac{x_2}{x_r}, \ldots, \frac{x_{r-1}}{x_r}, 1, \frac{x_{r+1}}{x_r}, \ldots, \frac{x_N}{x_r}\right),$$

where $|\frac{x_j}{x_r}| \leqslant 1$ for all j. Equating component r on both sides of the eigenvalue equation $Wx' = \lambda_1 x'$ gives

$$\lambda_1(W) = \sum_{j=1}^{N} w_{rj}\frac{x_j}{x_r} \leqslant \sum_{j=1}^{N}\left|w_{rj}\frac{x_j}{x_r}\right| \leqslant \sum_{j=1}^{N}|w_{rj}| = s_r,$$

when none of the elements of matrix W are negative. Since any component of x may have the largest modulus, $\lambda_1(W) \leqslant \max s_r$. ∎

2. Proof of Theorem 7

We consider the $2N \times 1$ vector z as $z^T = [\,C_1 x^T \;\; C_2 y^T\,]$ the linear combination of the principal eigenvector x and y of the two individual networks, respectively, where $x^T x = 1$, $y^T y = 1$, $C_1^2 + C_2^2 = 1$ such that $z^T z = 1$ and compute

$$\begin{aligned} z^T W z &= [C_1 x^T C_2 y^T]\begin{bmatrix} A_1 & \alpha B_{12} \\ \alpha B_{12}^T & A_2 \end{bmatrix}\begin{bmatrix} C_1 x \\ C_2 y \end{bmatrix} \\ &= C_1^2 x^T A_1 x + C_2^2 y^T A_2 y + 2\alpha 2 C_1 C_2 x^T B_{12} y \\ &= C_1^2 \lambda_1(A_1) + C_2^2 \lambda_1(A_2) + 2C_1 C_2 \xi, \end{aligned}$$

where $\xi = \alpha x^T B_{12} y$. By Rayleigh's principle $\lambda_1(W) \geqslant \frac{z^T W z}{z^T z} = z^T W z$. We could improve this lower bound by selecting z as the best linear combination (C_1 and C_2) of x and y. Let λ_L be the best possible lower bound $\frac{z^T W z}{z^T z}$ via the optimal linear combination of x and y. Thus,

$$\lambda_L = \max_{C_1^2 + C_2^2 = 1} C_1^2 \lambda_1(A_1) + C_2^2 \lambda_1(A_2) + 2C_1 C_2 \xi.$$

We use the Lagrange multipliers method and define the Lagrange function as

$$\Lambda = C_1^2 \lambda_1(A_1) + C_2^2 \lambda_1(A_2) + 2C_1 C_2 \xi - \mu\left(C_1^2 + C_2^2 - 1\right),$$

where μ is the Lagrange multiplier. The maximum is achieved at the solutions of

$$\begin{aligned} \frac{\partial \Lambda}{\partial C_1} &= 2C_1\lambda_1(A_1) + 2C_2\xi - 2C_1\mu = 0, \\ \frac{\partial \Lambda}{\partial C_2} &= 2C_2\lambda_1(A_2) + 2C_1\xi - 2C_2\mu = 0, \\ \frac{\partial \Lambda}{\partial \mu} &= C_1^2 + C_2^2 - 1 = 0. \end{aligned}$$

Note that $(C_1 \frac{\partial \Lambda}{\partial C_1} + C_2 \frac{\partial \Lambda}{\partial C_2})/2 = \lambda_L - \mu = 0$, which leads to $\mu = \lambda_L$. Hence, the maximum λ_L is achieved at the solution of

$$\begin{aligned} C_1\lambda_1(A_1) + C_2\xi - C_1\lambda_L = 0, \\ C_2\lambda_1(A_2) + C_1\xi - C_2\lambda_L = 0, \end{aligned}$$

that is,

$$\det\begin{pmatrix}\lambda_1(A_1)-\lambda_L & \xi\\ \xi & \lambda_1(A_2)-\lambda_L\end{pmatrix}=0.$$

This leads to

$$\begin{aligned}\lambda_L &= \frac{\lambda_1(A_1)+\lambda_1(A_2)}{2}+\sqrt{\left(\frac{\lambda_1(A_1)-\lambda_1(A_2)}{2}\right)^2+\xi^2}\\ &= \frac{\lambda_1(A_1)+\lambda_1(A_2)}{2}+\left|\frac{\lambda_1(A_1)-\lambda_1(A_2)}{2}\right|+\left(\sqrt{\left(\frac{\lambda_1(A_1)-\lambda_1(A_2)}{2}\right)^2+\xi^2}-\left|\frac{\lambda_1(A_1)-\lambda_1(A_2)}{2}\right|\right)\\ &= \max\left(\lambda_1(A_1),\lambda_1(A_2)\right)+\left(\sqrt{\left(\frac{\lambda_1(A_1)-\lambda_1(A_2)}{2}\right)^2+\xi^2}-\left|\frac{\lambda_1(A_1)-\lambda_1(A_2)}{2}\right|\right).\end{aligned}$$

The maximum is obtained when

$$z^T=\pm\left[\sqrt{\tfrac{\lambda_1(A_2)-\lambda_L}{\lambda_1(A_1)+\lambda_1(A_2)-2\lambda_L}}x^T\ \sqrt{\tfrac{\lambda_1(A_1)-\lambda_L}{\lambda_1(A_1)+\lambda_1(A_2)-2\lambda_L}}y^T\right].$$

3. Proof of Theorem 8

By Rayleigh's principle $\lambda_1^2(W)\geqslant\frac{z^TW^2z}{z^Tz}=z^TW^2z$. We consider z as linear combination $z^T=[\,{}_{C_1x^T}\ {}_{C_2y^T}\,]$ of x and y. The lower bound,

$$\begin{aligned}z^TW^2z &= [C_1x^T\ C_2y^T]\begin{bmatrix}A_1^2+\alpha^2B_{12}B_{12}^T & \alpha(A_1B_{12}+B_{12}A_2)\\ \alpha(A_1B_{12}+B_{12}A_2)^T & A_2^2+\alpha^2B_{12}^TB_{12}\end{bmatrix}\begin{bmatrix}C_1x\\ C_2y\end{bmatrix}\\ &= C_1^2x^TA_1^2x+C_2^2y^TA_2^2y+\alpha^2\left(C_1^2x^TB_{12}B_{12}^Tx+C_2^2y^TB_{12}^TB_{12}y\right)+2\alpha C_1C_2x^T(A_1B_{12}+B_{12}A_2)y\\ &= C_1^2\lambda_1^2(A_1)+C_2^2\lambda_1^2(A_2)+2C_1C_2\theta+\alpha^2\left(C_1^2\left\|B_{12}^Tx\right\|_2^2+C_2^2\left\|B_{12}y\right\|_2^2\right),\end{aligned}$$

where $\theta=\alpha(\lambda_1(A_1)+\lambda_1(A_2))x^TB_{12}y$. Let λ_L be the best possible lower bound z^TW^2z via the optimal linear combination (C_1 and C_2) of x and y. Thus,

$$\lambda_L=\max_{C_1^2+C_2^2=1}C_1^2\lambda_1^2(A_1)+C_2^2\lambda_1^2(A_2)+2C_1C_2\theta+\alpha^2\left(C_1^2\left\|B_{12}^Tx\right\|_2^2+C_2^2\left\|B_{12}y\right\|_2^2\right).$$

We use the Lagrange multipliers method and define the Lagrange function as

$$\Lambda=C_1^2\lambda_1^2(A_1)+C_2^2\lambda_1^2(A_2)+2C_1C_2\theta+\alpha^2\left(C_1^2\left\|B_{12}^Tx\right\|_2^2+C_2^2\left\|B_{12}y\right\|_2^2\right)-\mu\left(C_1^2+C_2^2-1\right),$$

where μ is the Lagrange multiplier. The maximum is achieved at the solutions of

$$\begin{aligned}\frac{\partial\Lambda}{\partial C_1} &= 2C_1\lambda_1^2(A_1)+2\alpha C_2\left(\lambda_1(A_1)+\lambda_1(A_2)\right)x^TB_{12}y+2\alpha^2C_1\left\|B_{12}^Tx\right\|_2^2-2C_1\mu=0,\\ \frac{\partial\Lambda}{\partial C_2} &= 2C_2\lambda_1^2(A_2)+2\alpha C_1\left(\lambda_1(A_1)+\lambda_1(A_2)\right)x^TB_{12}y+2\alpha^2C_2\left\|B_{12}y\right\|_2^2-2C_2\mu=0,\\ \frac{\partial\Lambda}{\partial\mu} &= C_1^2+C_2^2-1=0,\end{aligned}$$

which lead to $(C_1\frac{\partial\Lambda}{\partial C_1}+C_2\frac{\partial\Lambda}{\partial C_2})/2=\lambda_L-\mu=0$. Hence, the maximum λ_L is achieved at the solution of

$$C_1\lambda_1^2(A_1)+C_2\theta+\alpha^2C_1\left\|B_{12}^Tx\right\|_2^2-C_1\lambda_L=0,\quad C_2\lambda_1^2(A_2)+C_1\theta+\alpha^2C_2\left\|B_{12}y\right\|_2^2-C_2\lambda_L=0,$$

that is,

$$\det\begin{pmatrix}\lambda_1^2(A_1)+\alpha^2\left\|B_{12}^Tx\right\|_2^2-\lambda_L & \theta\\ \theta & \lambda_1^2(A_2)+\alpha^2\left\|B_{12}y\right\|_2^2-\lambda_L\end{pmatrix}=0.$$

This leads to

$$\lambda_L^2-\left(\lambda_1^2(A_1)+\alpha^2\left\|B_{12}^Tx\right\|_2^2+\lambda_1^2(A_2)+\alpha^2\left\|B_{12}y\right\|_2^2\right)\lambda_L+\left(\lambda_1^2(A_1)+\alpha^2\left\|B_{12}^Tx\right\|_2^2\right)\left(\lambda_1^2(A_2)+\alpha^2\left\|B_{12}y\right\|_2^2\right)-\theta^2=0.$$

Hence,

$$\lambda_L = \frac{\left(\lambda_1^2(A_1) + \alpha^2 \left\| B_{12}^T x \right\|_2^2 + \lambda_1^2(A_2) + \alpha^2 \| B_{12} y \|_2^2\right)}{2} + \frac{\sqrt{\left(\lambda_1^2(A_1) + \alpha^2 \left\| B_{12}^T x \right\|_2^2 + \lambda_1^2(A_2) + \alpha^2 \| B_{12} y \|_2^2\right)^2 - 4\left(\left(\lambda_1^2(A_1) + \alpha^2 \left\| B_{12}^T x \right\|_2^2\right)\left(\lambda_1^2(A_2) + \alpha^2 \| B_{12} y \|_2^2\right) - \theta^2\right)}}{2}$$

$$= \frac{\left(\lambda_1^2(A_1) + \alpha^2 \left\| B_{12}^T x \right\|_2^2 + \lambda_1^2(A_2) + \alpha^2 \| B_{12} y \|_2^2\right)}{2} + \sqrt{\left(\frac{\lambda_1^2(A_1) + \alpha^2 \left\| B_{12}^T x \right\|_2^2 - \lambda_1^2(A_2) - \alpha^2 \| B_{12} y \|_2^2}{2}\right)^2 + \theta^2},$$

which is obtained when

$$C_1 = \frac{\theta}{\sqrt{\theta^2 + \left(\lambda_L - \lambda_1^2(A_1) - \alpha^2 \left\| B_{12}^T x \right\|_2^2\right)^2}}, \quad C_2 = \frac{\lambda_L - \lambda_1^2(A_1) - \alpha^2 \left\| B_{12}^T x \right\|_2^2}{\sqrt{\theta^2 + \left(\lambda_L - \lambda_1^2(A_1) - \alpha^2 \left\| B_{12}^T x \right\|_2^2\right)^2}}.$$

4. Proof of Theorem 9

Any vector z of size $2N$ with $zz^T = m$ can be expressed as a linear combination of the eigenvectors $(z_1, z_2, \ldots, z_{2N})$ of matrix W,

$$\frac{z}{\sqrt{m}} = \sum_{i=1}^{2N} c_i z_i,$$

where $\sum_{i=1}^{2N} c_i^2 = 1$. Hence,

$$\frac{z^T W^s z}{z^T z} = \left(\sum_{i=1}^{2N} c_i z_i\right)^T \left(\sum_{i=1}^{2N} c_i W^s z_i\right) = \left(\sum_{i=1}^{2N} c_i z_i\right)^T \left(\sum_{i=1}^{2N} c_i \lambda_i^s z_i\right) = \sum_{i=1}^{2N} c_i^2 \lambda_i^k = \lambda_1^s \left(\sum_{i=1}^{2N} c_i^2 \frac{\lambda_i^s}{\lambda_1^k}\right).$$

Hence,

$$\lim_{k\to\infty} \left(\frac{z^T W^k z}{z^T z}\right)^{1/k} = \lambda_1(W).$$

According to Lyapunov's inequality,

$$(E[|X|^s])^{1/s} \leqslant (E[|X|^t])^{1/t},$$

when $0 < s < t$. Taking $\Pr[X = \frac{\lambda_i}{\lambda_1}] = c_i^2$, we have

$$\sum_{i=1}^{2N} c_i^2 \frac{\lambda_i^s}{\lambda_1^s} \leqslant \sum_{i=1}^{2N} c_i^2 \left|\frac{\lambda_i}{\lambda_1}\right|^s = (E[|X|^s])^{1/s} \leqslant (E[|X|^k])^{1/k} = \sum_{i=1}^{2N} c_i^2 \frac{\lambda_i^k}{\lambda_1^k},$$

since k is even and $k > s > 0$.

5. Proof of Theorem 10

$$\begin{aligned}\lambda_1(W) &= \max_{x^T x + y^T y = 1} [x^T y^T](A + \alpha B)\begin{bmatrix} x \\ y \end{bmatrix} \\ &= \max_{x^T x + y^T y = 1} \left([x^T y^T] A \begin{bmatrix} x \\ y \end{bmatrix} + \alpha\, [x^T y^T] B \begin{bmatrix} x \\ y \end{bmatrix}\right) \\ &\leqslant \max_{x^T x + y^T y = 1} (x^T A_1 x + y^T A_2 y) \\ &\quad + \alpha \max_{x^T x + y^T y = 1} [x^T y^T] B \begin{bmatrix} x \\ y \end{bmatrix} \\ &= \max(\lambda_1(A_1), \lambda_1(A_2)) + \alpha \lambda_1(B).\end{aligned}$$

The inequality is due to the fact that the two terms are maximized independently. The second term,

$$\begin{aligned}\lambda_1(B) &= \max_{x^T x + y^T y = 1} \left(x^T B_{12} y + y^T B_{12}^T x\right) \\ &= 2 \max_{x^T x + y^T y = 1} x^T B_{12} y,\end{aligned}$$

is equivalent to the system of equations,

$$B_{12} y = \lambda_1(B) x, \quad B_{12} y = \lambda_1(B) x, \quad x^T x + y^T y = 1,$$

or

$$B_{12}^T B_{12} y = \lambda_1(B)^2 y, \quad B_{12} B_{12}^T x = \lambda_1(B)^2 x, \quad x^T x + y^T y = 1,$$

which is to find the maximum eigenvalue (or more precisely the positive square root) of the symmetric positive matrix $B_{12} B_{12}^T$,

$$\lambda_1(B) = \sqrt{\max_{x^2=1} x^T B_{12} B_{12}^T x}.$$

This actually proves Lemma 3, the property $\lambda_1(B) = \sqrt{\lambda_1(B_{12} B_{12}^T)}$ of a bipartite graph B.

6. Proof of Theorem 11

The explicit expression up to the second order reads

$$\begin{aligned}&(A + \alpha B)(z^{(0)} + \alpha z^{(1)} + \alpha^2 z^{(2)} + O(\alpha^3)) \\ &= (\lambda^{(0)} + \alpha \lambda^{(1)} + \alpha^2 \lambda^{(2)} + O(\alpha^3)) \\ &\quad \times (z^{(0)} + \alpha z^{(1)} + \alpha^2 z^{(2)} + O(\alpha^3)). \qquad \text{(A1)}\end{aligned}$$

The zero-order expansion is simply

$$Az^{(0)} = \lambda^{(0)} z^{(0)}.$$

The problem at zero order becomes to find the maximum of

$$\frac{z^{(0)T} A z^{(0)}}{z^{(0)T} z^{(0)}} = \frac{(z^{(0)}, Az^{(0)})}{(z^{(0)}, z^{(0)})}.$$

In the nondegenerate case,

$$\max \frac{(z^{(0)}, Az^{(0)})}{(z^{(0)}, z^{(0)})} = \frac{(x, A_1 x)}{(x,x)} = \lambda_1(A_1).$$

Hence,

$$\lambda^{(0)} = \lambda_1(A_1), \quad (z^{(0)})^T = [x^T, \mathbf{0}^T],$$

where the first N elements of $z^{(0)}$ are x and the rest N elements are all zeros. Let us look at the first-order correction. Imposing the identity for the first-order expansion in (A1) gives

$$Az^{(1)} + Bz^{(0)} = \lambda^{(0)} z^{(1)} + \lambda^{(1)} z^{(0)}. \tag{A2}$$

Furthermore, we impose the normalization condition to z [see (6)], which leads to

$$(z^{(0)}, z^{(1)}) = 0. \tag{A3}$$

The first-order correction to the principal eigenvector is orthogonal to the zero order. Plugging this result in (A2),

$$(z^{(0)}, Az^{(1)} + Bz^{(0)}) = \lambda^{(0)}(z^{(0)}, z^{(1)}) + \lambda^{(1)}(z^{(0)}, z^{(0)}),$$
$$(A^T z^{(0)}, z^{(1)}) + (z^{(0)}, Bz^{(0)}) = \lambda^{(1)},$$

that is,

$$(z^{(0)}, Bz^{(0)}) = \lambda^{(1)}. \tag{A4}$$

Since $(z^{(0)})^T = (x^T \ \mathbf{0}^T)$ and $B = \left[\begin{smallmatrix} \mathbf{0} & B_{12} \\ B_{12}^T & \mathbf{0} \end{smallmatrix}\right]$, the first-order correction in this nondegenerate case is null $\lambda^{(1)} = 0$. Equation (A2) allows us to calculate also the first-order correction to the eigenvector,

$$Az^{(1)} + Bz^{(0)} = \lambda^{(0)} z^{(1)}, \quad (A - \lambda^{(0)} I) z^{(1)} = -Bz^{(0)}.$$

$(A - \lambda^{(0)} I)$ is invertible out of its kernel $(A - \lambda^{(0)} I)z = \mathbf{0}$ (that is the linear space generated by $z^{(0)}$) and since $Bz^{(0)} \perp z^{(0)}$ we have

$$z^{(1)} = (\lambda^{(0)} I - A)^{-1} Bz^{(0)}. \tag{A5}$$

Let us look for the second-order correction. Imposing the identification of the second-order term of (A1) we obtain

$$Az^{(2)} + Bz^{(1)} = \lambda^{(0)} z^{(2)} + \lambda^{(1)} z^{(1)} + \lambda^{(2)} z^{(0)}.$$

Projecting this vectorial equation on $z^{(0)}$ provides the second-order correction to λ,

$$\begin{aligned}
&(z^{(0)}, Az^{(2)} + Bz^{(1)}) \\
&\quad = \lambda^{(0)}(z^{(0)}, z^{(2)}) + \lambda^{(1)}(z^{(0)}, z^{(1)}) + \lambda^{(2)}(z^{(0)}, z^{(0)}), \\
\lambda^{(2)} &= (z^{(0)}, Az^{(2)}) + (z^{(0)}, Bz^{(1)}) - \lambda^{(0)}(z^{(0)}, z^{(2)}) \\
&= \lambda^{(0)}(z^{(0)}, z^{(2)}) + (z^{(0)}, Bz^{(1)}) - \lambda^{(0)}(z^{(0)}, z^{(2)}) \\
&= (z^{(0)}, Bz^{(1)}).
\end{aligned}$$

Substituting (A5) gives

$$\lambda^{(2)} = (z^{(0)}, B(\lambda^{(0)} I - A)^{-1} Bz^{(0)}), \tag{A6}$$

which can be further expressed as a function of the largest eigenvalue and eigenvector of individual network A_1, A_2 or their interconnections B_{12}. Since

$$Bz^{(0)} = \begin{pmatrix} 0 & B_{12} \\ B_{12}^T & 0 \end{pmatrix} \begin{pmatrix} x \\ 0 \end{pmatrix} = \begin{pmatrix} 0 \\ B_{12}^T x \end{pmatrix},$$

we have

$$\begin{aligned}
\lambda^{(2)} &= (B^T z^{(0)}, (\lambda^{(0)} I - A)^{-1} Bz^{(0)}) \\
&= (0 B_{12} x) \begin{pmatrix} (\lambda^{(0)} I - A_1) & 0 \\ 0 & (\lambda^{(0)} I - A_2) \end{pmatrix}^{-1} \begin{pmatrix} 0 \\ B_{12}^T x \end{pmatrix} \\
&= (0 x^T B_{12}) \begin{pmatrix} (\lambda^{(0)} I - A_1) & 0 \\ 0 & (\lambda^{(0)} I - A_2) \end{pmatrix}^{-1} \begin{pmatrix} 0 \\ B_{12}^T x \end{pmatrix} \\
&= (0 x^T B_{12}) \begin{pmatrix} (\lambda^{(0)} I - A_1)^{-1} & 0 \\ 0 & (\lambda^{(0)} I - A_2)^{-1} \end{pmatrix} \begin{pmatrix} 0 \\ B_{12}^T x \end{pmatrix} \\
&= x^T B_{12} (\lambda^{(0)} I - A_2)^{-1} B_{12}^T x,
\end{aligned}$$

which finishes the proof.

7. Proof of Theorem 12

The zero-order correction $z^{(0)} = \left[\begin{smallmatrix} x^{(0)} \\ y^{(0)} \end{smallmatrix}\right]$ of the principal eigenvector of W is a vector of size $2N$, with the first N elements denoted as vector $x^{(0)}$ and the last N elements denoted as $y^{(0)}$. Similarly, $z^{(1)} = \left[\begin{smallmatrix} x^{(1)} \\ y^{(1)} \end{smallmatrix}\right]$. In the degenerate case, the solution $z^{(0)}$ of the zero-order expansion equation,

$$Az^{(0)} = \lambda^{(0)} z^{(0)},$$

can be any combination of the principal eigenvector x and y of the two individual networks:

$$x^{(0)} = c_1 x, \quad y^{(0)} = c_2 y, \quad c_1^2 + c_2^2 = 1,$$

and $\lambda^{(0)} = \lambda_1(A_1) = \lambda_1(A_2)$. The first-order correction of the largest eigenvalue in the nondegenerate case (A4) holds as well for the degenerate case,

$$(z^{(0)}, Bz^{(0)}) = \lambda^{(1)}, \tag{A7}$$

which is however nonzero in the degenerate case due to the structure of $z^{(0)}$ and is maximized by the right choice of c_1 and c_2. Thus,

$$\begin{aligned}
\lambda_1(W) &= \max_{c_1, c_2} (\lambda_1(A_1) + \alpha(z^{(0)}, Bz^{(0)})) + O(\alpha^2) \\
&= \lambda_1(A_1) + \max_{c_1, c_2} \alpha c_1 c_2 \big((B_{12} y, x) + \big(B_{12}^T x, y\big)\big) + O(\alpha^2) \\
&= \lambda_1(A_1) + \tfrac{1}{2}\alpha \big((B_{12} y, x) + \big(B_{12}^T x, y\big)\big) + O(\alpha^2) \\
&= \lambda_1(A_1) + \alpha(x, B_{12} y) + O(\alpha^2),
\end{aligned}$$

where $c_1 c_2$ is maximum when $c_1 = c_2 = 1/\sqrt{2}$. Hence, $z^{(0)} = \left[\begin{smallmatrix} x^{(0)} \\ y^{(0)} \end{smallmatrix}\right] = \frac{1}{\sqrt{2}} \left[\begin{smallmatrix} x \\ y \end{smallmatrix}\right]$.

One may also evaluate the second-order correction $\lambda^{(2)}$ of the largest eigenvalue. The following results we derived in the nondegenerate case hold as well for the degenerate case,

$$\lambda^{(2)} = (z^{(0)}, Bz^{(1)})$$
$$Az^{(1)} + Bz^{(0)} = \lambda^{(0)} z^{(1)} + \lambda^{(1)} z^{(0)}.$$

The second equation allows us to calculate the first-order correction $z^{(1)}$ to the principal eigenvector:

$$(\lambda^{(0)}I - A)z^{(1)} = (B - \lambda^{(1)}I)z^{(0)}. \tag{A8}$$

This linear equation has solution when $(B - \lambda^{(1)}I)z^{(0)}$ is orthogonal to the kernel of the adjoint matrix of $\lambda^{(0)}I - A$, where the kernel is defined as

$$\mathrm{Ker}(\lambda^{(0)}I - A) = \{v : (\lambda^{(0)}I - A)v = 0\}.$$

First, we are going to prove that $(B - \lambda^{(1)}I)z^{(0)}$ is orthogonal to the kernel v. We assume that the largest eigenvalue is unique thus differs from the second largest eigenvalue in each single network A_1 and A_2, as observed in most complex networks. In this case,

$$A_1x^{(0)} = \lambda^{(0)}x^{(0)}$$
$$A_2y^{(0)} = \lambda^{(0)}y^{(0)}.$$

The kernel of the matrix $\lambda^{(0)}I - A$ is the linear space generated by $x^{(0)}$ and $y^{(0)}$

$$v = \begin{pmatrix} ax^{(0)} \\ by^{(0)} \end{pmatrix}.$$

Combining (A7), we have

$$v^T(B - \lambda^{(1)}I)z^{(0)} = a\left(\left(B_{12}^Tx^{(0)}, y^{(0)}\right) - \lambda^{(1)}\right) + b((x^{(0)}, B_{12}y^{(0)}) - \lambda^{(1)}) = 0.$$

Therefore, the solution of $z^{(1)}$ in (A8) exists.

Secondly, we will prove that all solutions of $z^{(1)}$ lead to the same $\lambda^{(2)}$. Any two solutions of $z^{(1)}$ differ by a vector in $\mathrm{Ker}(\lambda^{(0)}I - A)$ and can be denoted by, for example, $z^{(1)} = \begin{pmatrix} x^{(1)} \\ y^{(1)} \end{pmatrix}$ and $\hat{z}^{(1)} = \begin{pmatrix} x^{(1)} \\ y^{(1)} \end{pmatrix} + \begin{pmatrix} ax^{(0)} \\ by^{(0)} \end{pmatrix}$ confined by the normalization condition (A3):

$$(x^{(0)})^Tx^{(1)} + (y^{(0)})^Ty^{(1)} = 0$$
$$(x^{(0)})^T(x^{(1)} + ax^{(0)}) + (y^{(0)})^T(y^{(1)} + by^{(0)}) = 0,$$

which leads to $a = -b$. The $\lambda^{(2)}$ and $\hat{\lambda}^{(2)}$ corresponding to the two solutions,

$$\lambda^{(2)} = \begin{pmatrix} B_{12}y^{(0)} \\ B_{12}^Tx^{(0)} \end{pmatrix}^T \begin{pmatrix} x^{(1)} \\ y^{(1)} \end{pmatrix},$$
$$\hat{\lambda}^{(2)} = \begin{pmatrix} B_{12}y^{(0)} \\ B_{12}^Tx^{(0)} \end{pmatrix}^T \begin{pmatrix} x^{(1)} + ax^{(0)} \\ y^{(1)} - ay^{(0)} \end{pmatrix},$$

are equal since

$$\hat{\lambda}^{(2)} = \lambda^{(2)} + a\left[(y^{(0)})^TB_{12}^Tx^{(0)} - (x^{(0)})^TB_{12}y^{(0)}\right] = \lambda^{(2)}.$$

Therefore, all solutions of $z^{(1)}$ lead to the same second-order correction $\lambda^{(2)}$ to the eigenvalue and we are allowed to select any specific solution. We choose one solution by imposing the orthogonality of $x^{(1)}$ with $x^{(0)}$ and $y^{(1)}$ with $y^{(0)}$. Equation (A8) in components reads

$$(\lambda^{(0)}I - A_1)x^{(1)} = B_{12}y^{(0)} - \lambda^{(1)}x^{(0)}$$
$$(\lambda^{(0)}I - A_2)y^{(1)} = B_{12}^Tx^{(0)} - \lambda^{(1)}y^{(0)}.$$

We could replace $\lambda^{(0)}I - A_1$ by $\lambda^{(0)}I - A_1 + x^{(0)}(x^{(0)})^T$ and replace $\lambda^{(0)}I - A_2$ by $\lambda^{(0)}I - A_2 + y^{(0)}(y^{(0)})^T$ since $x^{(0)}$ is orthogonal with $x^{(1)}$ and $y^{(0)}$ is orthogonal with $y^{(1)}$:

$$(\lambda^{(0)}I - A_1 + x^{(0)}(x^{(0)})^T)x^{(1)} = B_{12}y^{(0)} - \lambda^{(1)}x^{(0)}$$
$$(\lambda^{(0)}I - A_2 + y^{(0)}(y^{(0)})^T)y^{(1)} = B_{12}^Tx^{(0)} - \lambda^{(1)}y^{(0)}.$$

This allows us to calculate $\lambda^{(2)}$ algebraically. The first-order correction $z^{(1)}$ to the principal eigenvector is

$$x^{(1)} = (\lambda^{(0)}I - A_1 + x^{(0)}(x^{(0)})^T)^{-1}(B_{12}y^{(0)} - \lambda^{(1)}x^{(0)})$$
$$y^{(1)} = (\lambda^{(0)}I - A_2 + y^{(0)}(y^{(0)})^T)^{-1}\left(B_{12}^Tx^{(0)} - \lambda^{(1)}y^{(0)}\right).$$

The second-order correction $\lambda^{(2)}$ of the largest eigenvalue follows:

$$\lambda^{(2)} = \begin{pmatrix} B_{12}y^{(0)} \\ B_{12}^Tx^{(0)} \end{pmatrix}^T \begin{pmatrix} (\lambda^{(0)}I - A_1 + x^{(0)}(x^{(0)})^T)^{-1} & 0 \\ 0 & (\lambda^{(0)}I - A_2 + y^{(0)}(y^{(0)})^T)^{-1} \end{pmatrix} \begin{pmatrix} B_{12}y^{(0)} - \lambda^{(1)}x^{(0)} \\ B_{12}^Tx^{(0)} - \lambda^{(1)}y^{(0)} \end{pmatrix},$$

which can be expressed as a function of the principal eigenvector x and y of each single network,

$$\lambda^{(2)} = \tfrac{1}{2}y^TB_{12}^T\left(\lambda^{(0)}I - A_1 + \tfrac{1}{2}xx^T\right)^{-1}(B_{12}y - \lambda^{(1)}x) + \tfrac{1}{2}x^TB_{12}\left(\lambda^{(0)}I - A_2 + \tfrac{1}{2}yy^T\right)^{-1}\left(B_{12}^Tx - \lambda^{(1)}y\right). \tag{A9}$$

[1] S. V. Buldyrev, R. Parshani, G. Paul, H. E. Stanley, and S. Havlin, Nature (London) **464**, 1025 (2010).

[2] E. A. Leicht and R. M. D'Souza, arXiv:0907.0894.

[3] R. Parshani, S. V. Buldyrev, and S. Havlin, Phys. Rev. Lett. **105**, 048701 (2010).

[4] J. Gao, S. V. Buldyrev, H. E. Stanley, and S. Havlin, Nature Physics **8**, 40 (2012).

[5] D. Zhou, H. E. Stanley, G. D'Agostino, and A. Scala, Phys. Rev. E **86**, 066103 (2012).

[6] X. Huang, S. Shao, H. Wang, S. V. Buldyrev, H. E. Stanley, and S. Havlin, Europhys. Lett. **101**, 18002 (2013).

[7] Q. Li, L. A. Braunstein, H. Wang, J. Shao, H. E. Stanley, and S. Havlin, J. Stat. Phys. **151**, 92 (2013).

[8] S. Funk and V. A. A. Jansen, Phys. Rev. E **81**, 036118 (2010).

[9] M. Dickison, S. Havlin, and H. E. Stanley, Phys. Rev. E **85**, 066109 (2012).

[10] A. Saumell-Mendiola, M. Ángeles Serrano, and M. Boguñá, Phys. Rev. E **86**, 026106 (2012).

[11] F. D. Sahneh, C. Scoglio, and F. N. Chowdhury, in *Proceedings of the 2013 American Control Conference*, *Washington, DC* (IEEE, 2013), pp. 2313–2318.

[12] R. M. Anderson and R. M. May, *Infectious Diseases of Humans* (Oxford University Press, Oxford, 1991).
[13] R. Pastor-Satorras and A. Vespignani, Phys. Rev. E **63**, 066117 (2001).
[14] S. C. Ferreira, C. Castellano, and R. Pastor-Satorras, Phys. Rev. E **86**, 041125 (2012).
[15] P. Van Mieghem, J. S. Omic, and R. E. Kooij, IEEE/ACM Transactions on Networking **17**, 1 (2009).
[16] P. Van Mieghem, *Graph Spectra for Complex Networks* (Cambridge University Press, Cambridge, 2011).
[17] M. Youssef and C. Scoglio, J. Theor. Biol. **283**, 136 (2011).
[18] J. G. Restrepo, E. Ott, and B. R. Hunt, Phys. Rev. E **71**, 036151 (2005).
[19] B. Bollobás, C. Borgs, J. Chayes, and O. Riordan, Ann. Probab. **38**, 150 (2010).
[20] E. Cator and P. Van Mieghem, Phys. Rev. E **85**, 056111 (2012).
[21] C. Li, R. van de Bovenkamp, and P. Van Mieghem, Phys. Rev. E **86**, 026116 (2012).
[22] O. Givan, N. Schwartz, A. Cygelberg, and L. Stone, J. Theor. Biol. **288**, 21 (2011).
[23] J. H. Wilkinson, *The Algebraic Eigenvalue Problem* (Oxford University Press, New York, 1965).
[24] P. Erdös and A. Rényi, Publ. Math. Inst. Hung. Acad. Sci. **5**, 17 (1960).
[25] P. Erdös and A. Rényi, Publ. Math. Debrecen **6**, 290 (1959).
[26] B. Bollobás, *Random Graphs* (Academic Press, London, 1985).
[27] A.-L. Barabási and R. Albert, Science **286**, 509 (1999).
[28] F. Chung, L. Lu, and V. Vu, Ann. Combin. **7**, 21 (2003).
[29] E. R. van Dam and W. H. Haemers, Discrete Math. **309**, 576 (2009).